Variational Pairing of Image Segmentation and Blind Restoration

Leah Bar[1], Nir Sochen[2], and Nahum Kiryati[1]

[1] School of Electrical Engineering
[2] Dept. of Applied Mathematics
Tel Aviv University, Tel Aviv 69978, Israel

Abstract. Segmentation and blind restoration are both classical problems, that are known to be difficult and have attracted major research efforts. This paper shows that the two problems are tightly coupled and can be successfully solved together. Mutual support of the segmentation and blind restoration processes within a joint variational framework is theoretically motivated, and validated by successful experimental results. The proposed variational method integrates Mumford-Shah segmentation with parametric blur-kernel recovery and image deconvolution. The functional is formulated using the Γ-convergence approximation and is iteratively optimized via the alternate minimization method. While the major novelty of this work is in the unified solution of the segmentation and *blind* restoration problems, the important special case of *known* blur is also considered and promising results are obtained.

1 Introduction

Image analysis systems usually operate on blurred and noisy images. The standard model $g = h * f + n$ is applicable to a large variety of image corruption processes that are encountered in practice. Here h represents an (often unknown) space-invariant blur kernel (point spread function), n is the noise and f is an ideal version of the observed image g.

The two following problems are at the basis of successful image analysis. (1) Can we segment g in agreement with the structure of f? (2) Can we estimate the blur kernel h and recover f? Segmentation and blind image restoration are both classical problems, that are known to be difficult and have attracted major research efforts, see e.g. [16, 3, 8, 9].

Had the correct segmentation of the image been known, blind image restoration would have been facilitated. Clearly, the blur kernel could have then been estimated based on the smoothed profiles of the known edges. Furthermore, denoising could have been applied to the segments without over-smoothing the edges. Conversely, had adequate blind image restoration been accomplished, successful segmentation would have been much easier to achieve. Segmentation and blind image restoration are therefore tightly coupled tasks: the solution of either problem would become fairly straightforward given that of the other.

This paper presents an integrated framework for simultaneous segmentation and blind restoration. As will be seen, strong arguments exist in favor of constraining the recovered blur kernel to parameterized function classes, see e.g. [4]. Our approach is presented in the context of the fundamentally important model of isotropic Gaussian blur, parameterized by its (unknown) width.

2 Fundamentals

2.1 Segmentation

The difficulty of image segmentation is well known. Successful segmentation requires top-down flow of models, concepts and a priori knowledge in addition to the image data itself. In their segmentation method, Mumford and Shah [10] introduced top-down information via the preference for piecewise-smooth segments separated by well-behaved contours. Formally, they proposed to minimize a functional that includes a fidelity term, a piecewise-smoothness term, and an edge integration term:

$$\mathcal{F}(f,K) = \frac{1}{2}\int_{\Omega}(f-g)^2 dA \; + \\ + \beta \int_{\Omega\setminus K} |\nabla f|^2 dA \; + \; \alpha \int_K d\sigma \tag{1}$$

Here K denotes the edge set and $\int_K d\sigma$ is the total edge length. The coefficients α and β are positive regularization constants. The primary difficulty in the minimization process is the presence of the unknown discontinuity set K in the integration domains.

The Γ-convergence framework approximates an irregular functional $\mathcal{F}(f,K)$ by a sequence $\mathcal{F}_\epsilon(f,K)$ of regular functionals such that

$$\lim_{\epsilon\to 0} \mathcal{F}_\epsilon(f,K) = \mathcal{F}(f,K)$$

and the minimizers of $\mathcal{F}_\epsilon$ approximate the minimizers of $\mathcal{F}$. Ambrosio and Tortorelli [1] applied this approximation to the Mumford-Shah functional, and represented the edge set by a characteristic function $(1-\chi_K)$ which is approximated by an auxiliary function v, i.e., $v(x) \approx 0$ if $x \in K$ and $v(x) \approx 1$ otherwise. The functional thus takes the form

$$\mathcal{F}_\epsilon(f,v) = \frac{1}{2}\int_{\Omega}(f-g)^2 dA \; + \; \beta \int_{\Omega} v^2 |\nabla f|^2 dA \; + \\ + \alpha \int_{\Omega} \left(\epsilon |\nabla v|^2 \; + \; \frac{1}{4\epsilon}(v-1)^2 \right) dA. \tag{2}$$

Richardson and Mitter [12] extended this formulation to a wider class of functionals. Discretization of the Mumford-Shah functional and its Γ-convergence approximation is considered in [5]. Additional perspectives on variational segmentation can be found in Vese and Chan [19] and in Samson *et al* [15].

Simultaneous segmentation and restoration of a blurred and noisy image has recently been presented in [7]. A variant of the Mumford-Shah functional was approached from a curve evolution perspective. In that work, the discontinuity set is limited to an isolated closed curve in the image and the blurring kernel h is assumed to be a priori known.

2.2 Restoration

Restoration of a blurred and noisy image is difficult even if the blur kernel h is known. Formally, finding f that minimizes

$$\|h * f - g\|^2_{L^2(\Omega)} \tag{3}$$

is an ill-posed inverse problem: small perturbations in the data may produce unbounded variations in the solution. In Tikhonov regularization [18], a smoothing term $\int_\Omega |\nabla f|^2 dA$ is added to the fidelity functional (3). In image restoration, Tikhonov regularization leads to over-smoothing and loss of important edge information. For better edge preservation, the Total Variation approach [13, 14] replaces L_2 smoothing by L_1 smoothing. The functional to be minimized is thus

$$\mathcal{F}(f,h) \;=\; \frac{1}{2}\|h * f - g\|^2_{L^2(\Omega)} \;+\; \beta \int_\Omega |\nabla f| dA \;. \tag{4}$$

This nonlinear optimization problem can be approached via the half-quadratic minimization technique [2]. An efficient alternative approach, based on the lagged diffusivity fixed point scheme and conjugate gradients iterations, was suggested by Vogel and Oman [20].

Image restoration becomes even more difficult if the blur kernel h is not known in advance. In addition to being ill-posed with respect to the image, the blind restoration problem is ill-posed in the kernel as well. To illustrate one aspect of this additional ambiguity, suppose that h represents isotropic Gaussian blur, with variance $\sigma^2 = 2t$:

$$h_t = \frac{1}{4\pi t} e^{-\frac{x^2+y^2}{4t}} \;.$$

The convolution of two Gaussian kernels is a Gaussian kernel, the variance of which is the sum of the two originating variances:

$$h_{t_1} * h_{t_2} = h_{t_1+t_2} \;. \tag{5}$$

Assume that the true t of the blur kernel is $t = T$, so $g = h_T * f$. The fidelity term (3) is obviously minimized by f and h_T. However, according to Eq. 5, g can also be expressed as

$$g = h_{t_1} * h_{t_2} * f \qquad \forall (t_1 + t_2) = T \;\;.$$

Therefore, an alternative hypothesis, that the original image was $h_{t_2} * f$ and the blur kernel was h_{t_1}, minimizes the fidelity term just as well. This exemplifies a

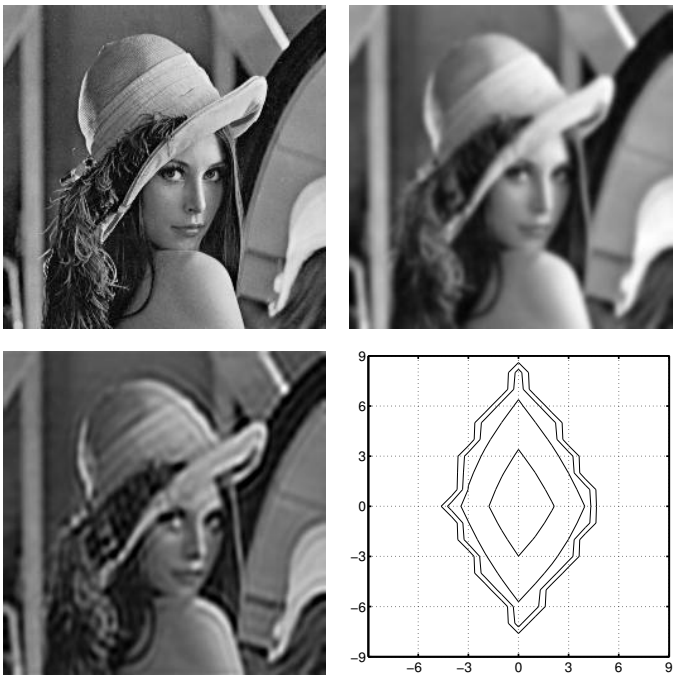

Fig. 1. Blind image restoration using the method of [6]. *Top-left:* Original. *Top-right:* Blurred using an isotropic Gaussian kernel ($\sigma = 2.1$). *Bottom-left:* Recovered image. *Bottom-right:* Reconstructed kernel.

fundamental ambiguity in the division of the apparent blur between the recovered image and the blur kernel, i.e., that the scene itself might be blurred. For meaningful image restoration, this hypothesis must be rejected and the largest possible blur should be associated with the blur kernel. It can be achieved by adding a kernel-smoothness term to the functional.

Blind image restoration with joint recovery of the image and the kernel, and regularization of both, was presented by You and Kaveh [21], followed by Chan and Wong [6]. Chan and Wong suggested to minimize a functional consisting of a fidelity term and total variation (L_1 norm) regularization for both the image and the kernel:

$$\mathcal{F}(f,h) \;=\; \frac{1}{2}\|h * f - g\|^2_{L^2(\Omega)} \;+\; \alpha_1 \int_\Omega |\nabla f| dA \;+\; \alpha_2 \int_\Omega |\nabla h| dA \;. \qquad (6)$$

Much can be learned about the blind image restoration problem by studying the characteristics and performance of this algorithm. Consider the images shown in Fig. 1. An original image (upper left) is degraded by isotropic Gaussian blur with $\sigma = 2.1$ (top-right). Applying the algorithm of [6] (with $\alpha_1 = 10^{-4}$ and $\alpha_2 = 10^{-4}$) yields a recovered image (bottom-left) and an estimated kernel

(bottom-right). It can be seen that the identification of the kernel is inadequate, and that the image restoration is sensitive to the kernel recovery error.

To obtain deeper understanding of these phenomena, we plugged the original image f and the degraded image g into the functional (6), and carried out minimization only with respect to h. The outcome was similar to the kernel shown in Fig. 1 (bottom-right). This demonstrates an excessive dependence of the recovered kernel on the image characteristics. At the source of this problem is the aspiration for general kernel recovery: the algorithm of [6] imposes only mild constraints on the shape of the reconstructed kernel. This allows the distribution of edge directions in the image to have an influence on the shape of the recovered kernel, via the trade-off between the fidelity and kernel smoothness terms. For additional insight see Fig. 2.

Facing the ill-posedness of blind restoration with a general kernel, two approaches can be taken. One is to add relevant data; the other is to constrain the solution. Recent studies have adopted one of these two approaches, or both. In [17], the blind restoration problem is considered within a multichannel framework, where *several* input images can be available.

In many practical situations, the blurring kernel can be modeled by the physics/optics of the imaging device and the set-up. The blurring kernel can then be constrained and described as a member in a class of parametric functions. This constraint was exploited in the direct blind deconvolution algorithm of [4]. In [11], additional relevant data was introduced via learning of similar images and the blur kernel was assumed to be Gaussian.

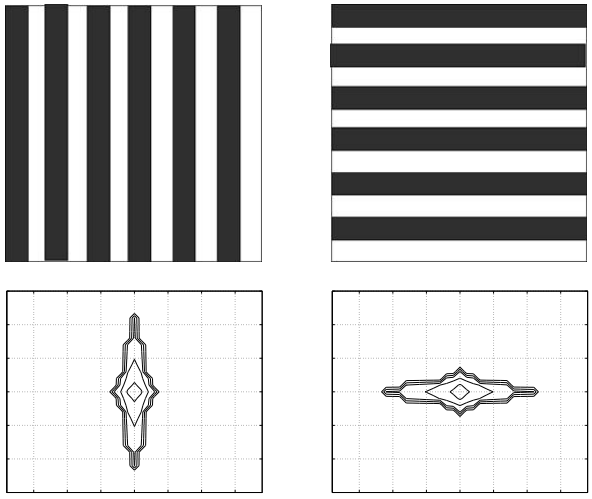

Fig. 2. Experimental demonstration of the dependence of the recovered kernel on the image characteristics in [6]. Each of the two synthetic bar images (top-row) was smoothed using an isotropic Gaussian kernel, and forwarded to the blind restoration algorithm of [6] (Eq. 6). The respective recovered kernels are shown in the bottom row.

3 Coupling segmentation with blind restoration

The observation, discussed in the introduction, that segmentation and blind restoration can be mutually supporting, is the fundamental motivation for this work. We present an algorithm, based on functional minimization, that iteratively alternates between segmentation, blur identification and restoration.

Concerning the sensitivity of general kernel recovery, we observe that large classes of practical imaging problems are compatible with reasonable constraints on the blur model. For example, Carasso [4] described the association of the Gaussian case with diverse applications such as undersea imaging, nuclear medicine, computed tomography scanners, and ultrasonic imaging in nondestructive testing.

In this work we integrate Mumford-Shah segmentation with blind deconvolution of isotropic Gaussian blur. This is accomplished by extending the Mumford-Shah functional and applying the Γ-convergence approximation as described in [1]. The observed image g is modeled as $g = h_\sigma * f + n$ where h_σ is an isotropic Gaussian kernel parameterized by its width σ, and n is white Gaussian noise. The objective functional used is

$$\mathcal{F}_\epsilon(f, h_\sigma, v) = \frac{1}{2}\int_\Omega (h_\sigma * f - g)^2 dA \; + \; \beta \int_\Omega v^2 |\nabla f|^2 dA \quad + \\ + \quad \alpha \int_\Omega \left(\epsilon |\nabla v|^2 \; + \; \frac{(v-1)^2}{4\epsilon} \right) dA + \gamma \int_\Omega |\nabla h_\sigma|^2 dA \qquad (7)$$

The functional depends on the functions f (ideal image) and v (edge integration map), and on the width parameter σ of the blur kernel h_σ. The first three terms are similar to the Γ-convergence formulation of the Mumford-Shah functional, as in (2). The difference is in the replacement of f in the fidelity term by the degradation model $h_\sigma * f$. The last term stands for the regularization of the kernel, necessary to resolve the fundamental ambiguity in the division of the apparent blur between the recovered image and the blur kernel. In the sequel it is assumed that the image domain Ω is a rectangle in $\mathbb{R}^2$ and that image intensities are normalized to the range $[0, 1]$.

Minimization with respect to f and v is carried out using the Euler-Lagrange equations (8) and (9). The differentiation by σ (10) minimizes the functional with respect to that parameter.

$$\frac{\delta \mathcal{F}_\epsilon}{\delta v} = 2\,\beta\, v\, |\nabla f|^2 + \alpha \left(\frac{v-1}{2\epsilon} \right) - 2\,\epsilon\,\alpha\,\nabla^2 v = 0 \qquad (8)$$

$$\frac{\delta \mathcal{F}_\epsilon}{\delta f} = (h_\sigma * f - g) * h_\sigma(-x, -y) - 2\beta\, \mathrm{Div}(v^2\, \nabla f) = 0 \qquad (9)$$

$$\frac{\partial \mathcal{F}_\epsilon}{\partial \sigma} = \int_\Omega \left[(h_\sigma * f - g) \left(\frac{\partial h_\sigma}{\partial \sigma} * f \right) + \gamma \frac{2h_\sigma^2}{\sigma^5} \left(\frac{x^2 + y^2}{\sigma^2} - 4 \right) \right] dA = 0 \qquad (10)$$

Studying the objective functional (7), it can be seen that it is convex and lower bounded with respect to any one of the functions f, v or h_σ if the other two

functions are fixed. For example, given v and σ, $\mathcal{F}_\epsilon$ is convex and lower bounded in f. Therefore, following [6], the alternate minimization (AM) approach can be applied: in each step of the iterative procedure we minimize with respect to one function and keep the other two fixed. The discretization scheme used was CCFD (cell-centered finite difference) [20]. This leads to the following algorithm:

`Initialization:` $f = g, \quad \sigma = \varepsilon_1, \quad v = 1, \quad \sigma_{prev} \gg 1$
`while` $(|\sigma_{prev} - \sigma| > \varepsilon_2)$ `repeat`

`1. Solve the Helmholtz equation for` v

$$(2\beta\,|\nabla f|^2 + \frac{\alpha}{2\epsilon} - 2\,\alpha\,\epsilon\,\nabla^2)\,v = \frac{\alpha}{2\epsilon}$$

`2. Solve the following linear system for` f

$$(h_\sigma * f - g) * h_\sigma(-x, -y) - 2\beta\,\mathrm{Div}(v^2\,\nabla f) = 0$$

`3. Set` $\sigma_{prev} = \sigma$`, and find` σ `such that (Eq. 10)`

$$\frac{\partial F_\epsilon}{\partial \sigma} = 0$$

Here ε_1 and ε_2 are small positive constants. Both steps 1 and 2 of the algorithm call for a solution of a system of linear equations. Step 1 was implemented using the Generalized Minimal Residual (GMRES) algorithm. In step 2, a symmetric positive definite operator is applied to $f(x, y)$. Implementation was therefore via the Conjugate Gradients method. In step 3, the derivative of the functional with respect to σ was analytically determined, and its zero crossing was found using the bisection method. All convolution procedures were performed in the Fourier Transform domain. The algorithm was implemented in MATLAB environment.

4 Special case: known blur kernel

If the blur kernel is known, the restriction to Gaussian kernels is no longer necessary. In this case, the kernel-regularization term in the objective functional (7) can be omitted. Consequently, the algorithm can be simplified by skipping step 3 and replacing the stopping criterion by a simple convergence measure.

The resulting algorithm for coupled segmentation and image restoration is fast, robust and stable. Unlike [7], the discontinuity set is not restricted to isolated closed contours. Its performance is exemplified in Fig. 3. The top-left image is a blurred and slightly noisy version of the original 256×256 *Lena* image (not shown). The blur kernel was a pill-box of radius 3.3. The top-right image is the reconstruction obtained using the Matlab's Image Processing Toolbox adaptation of the Lucy-Richardson algorithm (`deconvlucy`). The bottom-left image is the outcome of the proposed method; the bottom-right image shows the associated edge map v determined by the algorithm ($\beta = 1$, $\alpha = 10^{-8}$, $\epsilon = 10^{-5}$, 4 iterations). Computing time was 2 minutes in interpreted MATLAB on a 2GHz PC. The superiority of the suggested method is clear.

Fig. 3. The case of a known blur kernel. *Top-left:* Corrupted image. *Top-right:* Restoration using the Lucy-Richardson algorithm (MATLAB: `deconvlucy`). *Bottom-left:* Restoration using the suggested method. *Bottom-right:* Edge map produced by the suggested method.

5 Results: segmentation with blind restoration

Consider the example shown in Fig. 4. The top-left image was obtained by blurring the original 256×256 *Lena* image (not shown) with a Gaussian kernel with $\sigma = 2.1$. The proposed method for segmentation and blind restoration was applied, with $\beta = 1$, $\gamma = 50$, $\alpha = 10^{-7}$ and $\epsilon = 10^{-4}$. The initial value of σ was $\varepsilon_1 = 0.5$ and the convergence tolerance was taken as $\varepsilon_2 = 0.001$. Convergence was achieved after 24 iterations; the unknown width of the blur kernel was estimated to be $\sigma = 2.05$, which is in pleasing agreement with its true value. The reconstructed image is shown top-right, and the associated edge map is presented at the bottom of Fig. 4. Compare to Fig. 1.

The top-left image in Fig. 5 is a 200×200 gray level image, synthetically blurred by an isotropic Gaussian kernel ($\sigma = 2.1$) and additive white Gaussian noise (SNR=44dB). Restoration using [6] ($\alpha_1 = 10^{-4}$, $\alpha_2 = 10^{-4}$) is shown top-right. The reconstruction using the method suggested in this paper ($\beta = 1$, $\alpha = 10^{-6}$, $\gamma = 20$, $\epsilon = 10^{-3}$) is shown bottom-left, and the associated edge map v is shown bottom-right. The number of iterations to convergence was 18, and the estimated width of the blur kernel was 1.9. The convergence process is illustrated in Fig. 6.

Fig. 4. Segmentation and blind restoration. *Top-left:* Blurred image ($\sigma = 2.1$). *Top-right:* Blind reconstruction using the proposed algorithm. *Bottom:* Edge map v produced by the suggested method. Compare to Fig. 1.

The last example refers to actual defocus blur. The top-left image in Fig. 7 is a 200×200 rescaled part of an image obtained with deliberate defocus blur, using a Canon VC-C1 PTZ video communication camera and SGI O2 analog video acquisition hardware. The shape and size of the actual defocus blur were not known to us; they certainly deviate from the isotropic Gaussian model. The top-right image in Fig. 7 shows the blind restoration result of [6] ($\alpha_1 = 10^{-4}$, $\alpha_2 = 10^{-6}$). At the bottom-left is the reconstruction using the method suggested in this paper ($\beta = 1$, $\alpha = 10^{-2}$, $\gamma = 100$, $\epsilon = 0.1$). Convergence was achieved within 7 iterations, and the blur kernel width was estimated to be 1.68. The edge map v is shown bottom-right. The quality of this result demonstrates the applicability of the proposed method to real images and its robustness to reasonable deviations from the Gaussian case. In all our experiments $\beta = 1$, and the best value of γ, controlling the deconvolution level, was in the range $20 \leq \gamma \leq 100$. The values of ϵ and α had to be increased in the presence of noise.

6 Discussion

This paper validates the hypothesis that the challenging tasks of image segmentation and blind restoration are tightly coupled. Mutual support of the seg-

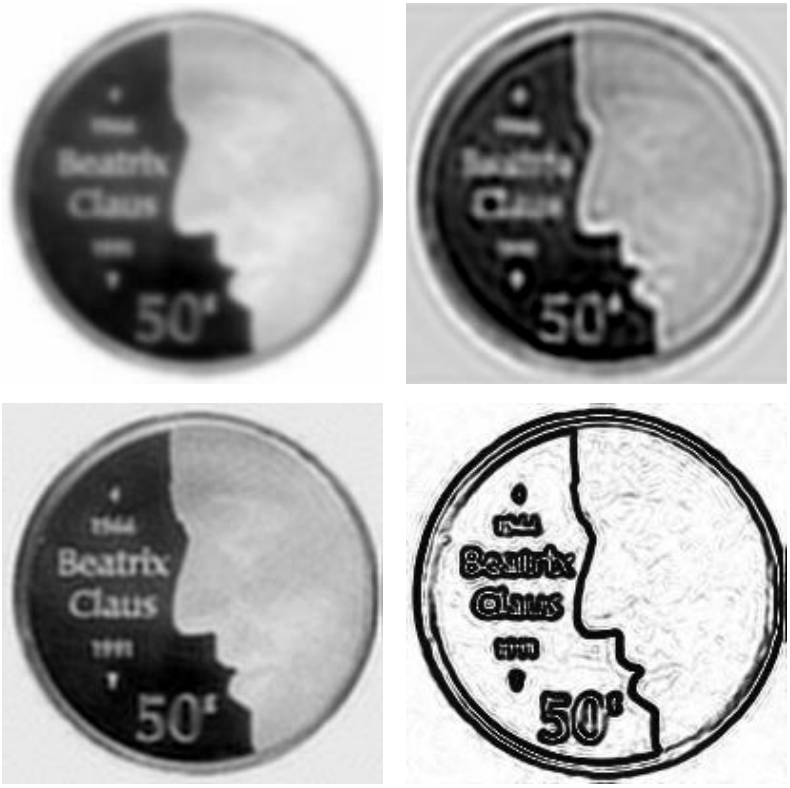

Fig. 5. Segmentation and blind restoration. *Top-left:* Blurred ($\sigma = 2.1$) image with slight additive noise. *Top-right:* Restoration using the method of [6]. *Bottom-left:* Restoration using the suggested method. *Bottom-right:* Edge map produced by the suggested method.

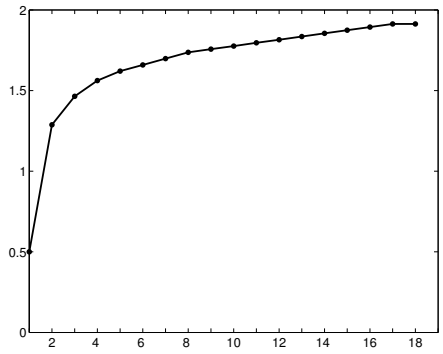

Fig. 6. The convergence of the estimated width σ of the blur kernel as a function of the iteration number in the blind recovery of the coin image.

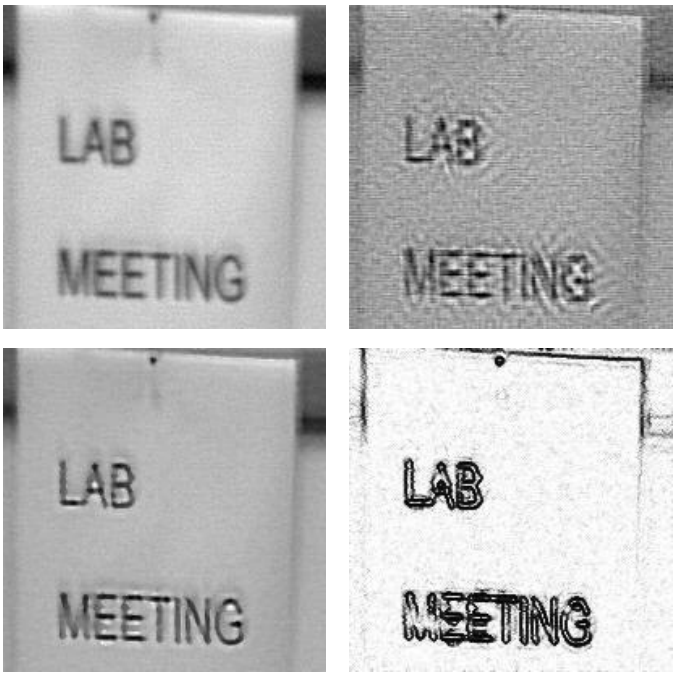

Fig. 7. Segmentation and blind restoration of unknown defocus blur. *Top-left:* Blurred image. *Top-right:* Restoration using the method of [6]. *Bottom-left:* Restoration using the suggested method. *Bottom-right:* Edge map produced by the suggested method.

mentation and blind restoration processes within an integrative framework is demonstrated.

Inverse problems in image analysis are difficult and often ill-posed. This means that searching for the solution in the largest possible space is not always the best strategy. A-priori knowledge should be used, wherever possible, to limit the search and constrain the solution. In the context of pure blind restoration, Carasso [4] analyzes previous approaches and presents convincing arguments in favor of restricting the class of blurs.

Along these lines, in this paper the blur kernels are constrained to the class of isotropic Gaussians parameterized by their width. This is a sound approximation of physical kernels encountered in diverse contexts [4]. The advantages brought by this restriction are well-demonstrated in the experimental results that we provide. We plan to extend this approach to parametric kernel classes to which the Gaussian approximation is inadequate, in particular, motion blur.

While the major novelty in this work is in the unified solution of the segmentation and *blind* restoration problems, we have obtained valuable results also in the case of *known* blur, see Fig. 3 (bottom-left). Note that if the blur is known, the restriction to the Gaussian case is no longer necessary.

References

1. L. Ambrosio and V.M. Tortorelli, "Approximation of Functionals Depending on Jumps by Elliptic Functionals via Γ-Convergence", *Communications on Pure and Applied Mathematics*, Vol. XLIII, pp. 999-1036, 1990.
2. G. Aubert and P. Kornprobst, *Mathematical Problems in Image Processing*, Springer, New York, 2002.
3. M. Banham and A. Katsaggelos, "Digital Image Restoration", *IEEE Signal Processing Mag.*, Vol. 14, pp. 24-41, 1997.
4. A. S. Carasso, "Direct Blind Deconvolution", *SIAM J. Applied Math.*, Vol. 61, pp. 1980-2007, 2001.
5. A. Chambolle, "Image Segmentation by Variational Methods: Mumford and Shah functional, and the Discrete Approximation", *SIAM Journal of Applied Mathematics*, Vol. 55, pp. 827-863, 1995.
6. T. Chan and C. Wong, "Total Variation Blind Deconvolution", *IEEE Trans. Image Processing*, Vol. 7, pp. 370-375, 1998.
7. J. Kim, A. Tsai, M. Cetin and A.S. Willsky, "A Curve Evolution-based Variational Approach to Simultaneous Image Restoration and Segmentation", *Proc. IEEE ICIP*, Vol. 1, pp. 109-112, 2002.
8. D. Kundur and D. Hatzinakos, "Blind Image Deconvolution", *Signal Processing Mag.*, Vol. 13, pp. 43-64, May 1996.
9. D. Kundur and D. Hatzinakos, "Blind Image Deconvolution Revisited", *Signal Processing Mag.*, Vol. 13, pp. 61-63, November 1996.
10. D. Mumford and J. Shah, "Optimal Approximations by Piecewise Smooth Functions and Associated Variational Problems", *Communications on Pure and Applied Mathematics*, Vol. 42, pp. 577-684, 1989.
11. R. Nakagaki and A. Katsaggelos, "A VQ-Based Blind Image Restoration Algorithm", *IEEE Trans. Image Processing*, Vol. 12, pp. 1044-1053, 2003.
12. T. Richardson and S. Mitter, "Approximation, Computation and Distortion in the Variational Formulation", in *Geometery-Driven Diffusion in Computer Vision*, B.M. ter Harr Romeny, Ed. Kluwer, Boston, 1994, pp. 169-190.
13. L. Rudin, S. Osher and E. Fatemi, "Non Linear Total Variation Based Noise Removal Algorithms", *Physica D*, Vol. 60, pp. 259-268, 1992.
14. L. Rudin and S. Osher, "Total Variation Based Image Restoration with Free Local Constraints", *Proc. IEEE ICIP*, Vol. 1, pp. 31-35, Austin TX, USA, 1994.
15. C. Samson, L. Blanc-Féraud, G. Aubert and J. Zerubia, "Multiphase Evolution and Variational Image Classification", *Technical Report No. 3662*, INRIA Sophia Antipolis, April 1999.
16. M. Sonka, V. Hlavac and R. Boyle, *Image Processing, Analysis and Machine Vision*, PWS Publishing, 1999.
17. F. Sroubek and J. Flusser, "Multichannel Blind Iterative Image Restoration", *IEEE. Trans. Image Processing*, Vol. 12, pp. 1094-1106, 2003
18. A. Tikhonov and V. Arsenin, "Solutions of Ill-posed Problems", New York, 1977.
19. L.A. Vese and T.F. Chan, "A Multiphase Level Set Framework for Image Segmentation Using the Mumford and Shah Model", *International Journal of Computer Vision*, Vol. 50, pp. 271-293, 2002.
20. C. Vogel and M. Oman, "Fast, Robust Total Variation-based Reconstruction of Noisy, Blurred Images", *IEEE Trans. Image Processing*, Vol. 7, pp. 813-824, 1998.
21. Y. You and M. Kaveh, "A Regularization Approach to Joint Blur Identification and Image Restoration", *IEEE Trans. Image Processing*, Vol. 5, pp. 416-428, 1996.